

# AS-1 attenuates the inflammatory response by targeting AKT and MAPK in LPS-activated acute lung injury models

Fuling Cen<sup>a,b</sup>, Yanmei Wei<sup>b</sup>, Xuan Zhang<sup>b</sup>, Hanmeng Liu<sup>b</sup>, Guangying Chen<sup>a,b,\*</sup>

<sup>a</sup> College of pharmacy, Fujian University of Traditional Chinese Medicine, Fuzhou 350000 China

<sup>b</sup> Key Laboratory of Tropical Medicinal Resource Chemistry of Ministry of Education, College of Chemistry and Chemical Engineering, Hainan Normal University, Haikou 571158 China

\*Corresponding author, e-mail: chgying123@163.com

Received 7 Jan 2025, Accepted 8 May 2025

Available online 15 Jun 2025

**ABSTRACT:** We investigated the effects of 3 $\alpha$ ,28-dihydroxyolean-12-ene (AS-1) on lipopolysaccharide (LPS)-induced acute lung injury (ALI) in Balb/c mice and attempted to elucidate its underlying mechanism of action. The levels of pro-inflammatory cytokines such as tumor necrosis factor- $\alpha$  (TNF- $\alpha$ ), interleukin-6 (IL-6), and interleukin-1 $\beta$  (IL-1 $\beta$ ) were measured using an ELISA kit. Furthermore, we analyzed the protein expression levels of inducible nitric oxide synthase (iNOS), cyclooxygenase-2 (COX-2), and the proteins involved in the kinase B/mitogen-activated protein kinase (AKT/MAPK) signaling pathways by Western blot analysis. Additionally, we evaluated AS-1 for toxicity and teratogenicity using the Cell Counting Kit-8 (CCK-8) assay and the zebrafish embryo toxicity assay. The results revealed that AS-1 suppressed the expression of pro-inflammatory cytokines and the phosphorylation of MAPK-related proteins, while enhancing the phosphorylation of AKT-related proteins. Furthermore, AS-1 was found to be non-teratogenic at concentrations below 12.5  $\mu$ M. These findings suggest that AS-1 may alleviate ALI by modulating the AKT/MAPK signaling pathway.

**KEYWORDS:** triterpenoid AS-1, zebrafish, acute lung injury, anti-inflammation, MAPK/AKT signaling pathway

## INTRODUCTION

ALI, a milder form of Acute Respiratory Distress Syndrome (ARDS), is also a condition of acute inflammation [1]. There is a large body of evidence that gram-negative bacterial infections are a major cause of ALI [2]. In addition, LPS, the major component of the outer membrane of gram-negative bacteria, can cause lung injury and inflammatory response [3]. Inflammation is a complex response in living tissues that protects our bodies by neutralizing dangerous pathogens, preventing infection, and promoting wound healing [4]. The release of pro-inflammatory factors—such as nitric oxide (NO), IL-1 $\beta$ , TNF- $\alpha$ , and IL-6—which act as important mediators accompanies this process [5]. Furthermore, inflammatory factors activate inflammation-related pathways, which in turn lead to the overexpression of relevant proteins and exacerbation of inflammation [6]. During the development of inflammation, the immune system is activated by the recognition of endotoxin antigens via Toll-like receptors (TLRs), which then activate antigen-induced pathways to recruit downstream proteins such as MAPKs and AKT [7]. MAPKs, including c-Jun N-activated kinase (JNK), extracellular signal-regulated kinase (ERK), and p38, are key cellular signaling pathways that are activated in response to stimulation by LPS [8]. AKT is a serine/threonine kinase. It is considered one of the major effector kinases downstream of PI3K and a major contributor to the PI3K/AKT signaling pathway [9]. PI3K/AKT signaling is activated downstream of multiple cell-surface receptors [10], regulating downstream

targets and cross-talking with other important signal transduction networks such as MAPK/extracellular signal-regulated kinase 1/2 (ERK1/2) signaling [11]. Fine-tuned crosstalk between PI3K/AKT and MAPK/ERK signaling is essential for cell homeostasis and is achieved through a feedback control loop, where activated ERK inhibits AKT phosphorylation and vice versa [12]. It has been suggested that these signaling pathways are involved in inflammation by regulating the expression of inflammation-related cytokines and enzymes such as cyclooxygenase (COX). Thus, targeting inflammation-related signaling pathways may be a beneficial way to slow the progression of inflammation and further improve ALI.

*Alangium salviifolium* is a member of the genus *Alangium* and the family Alangiaceae [13]. Every part of this plant is mentioned in Ayurveda and traditional medicine for the treatment of various ailments. Among these, the leaves are used to treat asthma and rheumatism [14]. However, the scientific evidence is lacking. Previous studies have reported hepatoprotective and anti-inflammatory activity against CCl<sub>4</sub>-induced liver damage in rats by the ethanolic extract of *A. salviifolium* leaves [15]. 3 $\alpha$ ,28-dihydroxyolean-12-ene (AS-1) is a triterpenoid compound extracted from the petroleum ether fraction of *A. salviifolium* leaves, which has shown excellent anti-inflammatory activity in previous studies conducted in our laboratory. Therefore, AS-1 may have the potential to impede the key cycle of cytokine secretion and inflammation, thereby providing a new therapeutically beneficial option for inflammation. However, it remains unclear

whether AS-1 has an anti-inflammatory effect on LPS-induced ALI. Thus, it is necessary not only to investigate whether AS-1 has a positive effect on ALI but also to clarify the potential underlying mechanisms.

## MATERIALS AND METHODS

### Experimental materials and reagents

Antibodies, iNOS (#13120), COX-2 (#12282), AKT (#9272), phospho-AKT (#4060), ERK (#4695), phospho-ERK (#4370), JNK (#9252), phospho-JNK (#4668), p38 (#8690), phospho-p38 (#4511), and GAPDH (#2118) primary antibodies as well as an anti-rabbit immunoglobulin G (IgG) secondary antibody, were purchased from Cell Signaling Technology (Boston, USA). LPS and dexamethasone (DEX, purity  $\geq 98\%$ ) were obtained from Sigma-Aldrich (St. Louis, USA). The compounds AS-1 were isolated by Dr. Yanmei Wei in Key Laboratory of Tropical Medicinal Resource Chemistry of Ministry of Education, Beijing, China).

### Mouse model

Male Balb/c mice (aged 8 weeks and weighing  $26 \pm 2$  g) were purchased from SPF Biotechnology Company (Beijing, China). The animal experiments were officially approved by the Animal Ethics Committee of Hainan Medical University (ethics number: HYLL-2024-243). Animals were kept in the housing facility for one week to adapt to the environment before the experiment and were maintained at  $24 \pm 1^\circ\text{C}$  under a 16/8 h light/dark cycle with food and water provided *ad libitum*. Six groups of animals were maintained in different cages with 10 mice per cage. The normal control group and LPS group were administered sesame oil + DMSO (below 1% (v/v)) via intraperitoneal injection. The positive control group was administered DEX (5 mg/kg/day) via intraperitoneal injection. The other 3 groups were administered AS-1 (dissolved in DMSO) via intraperitoneal injection (1.5, 3, and 6 mg/kg/day). The intraperitoneal injection administration continued for 7 days. One day before sampling the Balb/c mice, the positive control group and the 3 AS-1 administered groups received bronchial injections with LPS (5 mg/kg/day). Animals were anesthetized by diethyl ether and sacrificed after the last LPS stimulation for 24 h. The trachea was cannulated with a 20-gauge blunt needle. Lungs were lavaged 3 times with 0.8 ml of ice-cold PBS (pH 7.4). BALF was centrifuged ( $4^\circ\text{C}$ ,  $1500 \times g$ , 10 min) to pellet cells. Lung tissue and bronchoalveolar lavage fluid (BALF) samples were collected and stored at  $-80^\circ\text{C}$  until further analysis.

### Cytokine ELISA analyses

Cytokine (IL-6, TNF- $\alpha$ , and IL-1 $\beta$ ) levels were estimated in mouse BALF using ELISA kits (Ray Biotech, Georgia, USA) according to the manufacturer's protocols. For IL-6 and TNF- $\alpha$  analysis, BALF was diluted

100-fold using sample standard dilutions. For IL-1 $\beta$ , BALF was not diluted. Briefly, samples were pipetted into a micro-plate pre-coated with capture antibodies and incubated at room temperature for 2 h. After 5 washes with wash buffer, HRP conjugated antibodies were added and incubated for 2 h at room temperature. Then, substrate solution was added, and the plates were incubated at room temperature in the dark for 30 min. The reaction was stopped by the stop solution, and the optical density of each well was measured at 450 nm with a microplate reader (BioTek Synergy H1, Winooski, USA).

### Western blot analysis

Total protein samples (50  $\mu\text{g}/\text{ml}$ ) were separated by sodium dodecyl sulfate-polyacrylamide gel electrophoresis (SDS-PAGE) with 10% acrylamide/bis gels and electrotransferred to Immobilon-P polyvinylidene difluoride (PVDF) membranes (Beyotime, Shanghai, China). The membranes were then blocked with Protein Free Rapid Sealing Solution (Epizyme, Wuhan, China) and incubated with secondary HRP-conjugated IgG (1:2000) at room temperature for 1 h. Protein bands were visualized using a chemiluminescence Western blot detection system (Analytik Jena, Jena, Germany).

### Cell culture

THP-1 human monocytes (ATCC, Manassas, VA, USA) were cultivated in THP-1 Cell Specialty Media (Procell, Wuhan, China). The monocytes were grown at  $37^\circ\text{C}$  in a humidified incubator maintained at 5%  $\text{CO}_2$  concentration.

### Cytotoxicity assay

Cell viability was assessed using the CCK-8 assay (Beyotime). THP-1 monocytes were uniformly seeded into 96-well plates at a density of  $1 \times 10^5$  monocytes/ml per well. Cells were then exposed to different concentrations of AS-1 (100, 50, 25, 12.5, 6.25, 3.125, and 1.56  $\mu\text{M}$ ) and incubated at  $37^\circ\text{C}$  and 5%  $\text{CO}_2$ . After incubating for 24 h, the proliferation activity of THP-1 monocytes was detected using CCK-8 kit. This procedure was strictly in accordance with the kit instructions to determine the toxicity range of AS-1 to THP-1 monocytes. According to the protocol, the optical density (OD) value of each well was detected at 450 nm using enzyme-labeled instrument (BioTek Synergy H1).

### Nitrite assay

The nitrite content in THP-1 monocytes was determined using the NO Fluorescence Kit (Beyotime). Briefly, THP-1 monocytes were evenly seeded into Nest glass 35mm confocal dishes at a density of  $3 \times 10^5$  cells/ml and cultured for 24 h. Following 24 h incubation, the THP-1 cells were differentiated using Phorbol

12-myristate 13-acetate (PMA) (Sigma-Aldrich). After differentiation, the monocytes were incubated with the drugs for 1 h, followed by exposure to LPS for an additional 23 h. According to the manufacturer's instructions, the monocytes were then loaded with the NO fluorescent probe and incubated at 37°C in a 5% CO<sub>2</sub> atmosphere for 30 min. Finally, the monocytes were observed under a Confocal Laser Scanning Microscope (OLYMPUS FV3000, Tokyo, Japan).

### Embryotoxicity assay

Wild-type (WT) adults were maintained under a 14/10 h light/dark cycle at 28°C. Ethics and permits: the experiments comply with the current laws of China. Experimental procedures were in accordance with the Animal Research Ethics Committee of Hainan Provincial Education Centre for Ecology and Environment, Hainan Normal University (No. HNECEE-2023-010). Embryos were gathered and developed in chorion water (0.5 mg/l methylene blue) for up to 120 h post-fertilization (hpf) at 28.5°C. Zebrafish embryos were randomly divided into 7 groups: the control group (raised in fish water), and 6 AS-1-treated groups. AS-1 was dissolved in DMSO and diluted with fish water to final concentrations of 3.125, 6.25, 12.5, 25, 50, and 100 µM. The embryos were incubated in 12-well plates at a density of 10 embryos per well for 120 hpf continuously and observed and photographed daily. In addition, the culture solution was changed every 48 hpf.

### Statistical analysis

Data are expressed as mean ± SEM of each independent replication. For comparison of 3 or more replications, data were analyzed by one-way analysis of variance (ANOVA) with Dunnett's post-hoc test. The value of  $p < 0.05$  was considered statistically significant. Statistical tests were performed using GraphPad Prism 5.0 (GraphPad Software).

## RESULTS

### Measurement of the pro-inflammation expression in ALI mice treated with different concentrations of AS-1

Following a 7-day pretreatment period with intraperitoneal administration of AS-1 at graded doses (1.5, 3, and 6 mg/kg), no mortality was observed in any experimental cohort. At 24 h post-LPS challenge, the model group exhibited characteristic inflammatory manifestations, including excessive corneal exudation, hypoactivity, and piloerection with diminished fur luster when compared to the blank control group. Notably, a dose-dependent attenuation of these pathological features was observed across AS-1 treatment groups with the high-dose AS-1 group (6 mg/kg) demonstrating symptom amelioration comparable to the pharmacological

intervention achieved by DEX (5 mg/kg) in the positive control group (Table S1). The effects of AS-1 on inflammation related factors including IL-1β, TNF-α, IL-6, and proteins iNOS and COX-2 were investigated. Compared with the LPS group, the contents of IL-6, IL-1β, and TNF-α in the BALF of mice treated with AS-1 (1.5, 3, or 6 µM) for 24 h were significantly reduced (Fig. 1b–d). Western blot results further demonstrated that iNOS and COX-2 expressions in mouse lung tissue were markedly inhibited (Fig. 1e–h).

### Measurement of the AKT/MAPK-related protein expression in ALI mice treated with different concentrations of AS-1

As illustrated in Fig. 2a,b, Western blot results in LPS-induced ALI mice demonstrated remarkable suppression of p-AKT. Notably, AS-1 significantly promoted the phosphorylation of AKT, indicating that AS-1 activated the AKT signaling pathway. The MAPK signaling pathway plays a crucial role in the regulation of many inflammatory responses. To investigate the participation of AS-1 in the molecular mechanism of the LPS-induced inflammatory response, JNK, ERK, and p38 protein phosphorylation were detected in ALI mice lung tissue. As shown in Fig. 2c–h, LPS treatment led to a significant increase in the phosphorylation of JNK, ERK, and p38 in ALI mice lung tissue. However, AS-1 treatment significantly attenuated the LPS-stimulated activation of JNK, ERK, and p38. These findings suggest that AS-1 may attenuate proinflammatory factors by inhibiting the MAPK signaling cascade and further alleviate the LPS-induced ALI inflammatory response by promoting AKT activation.

### Measurement of the toxicity and NO expression in THP-1 monocytes treated with different concentrations of AS-1

THP-1 was treated with various concentrations of AS-1 (100, 50, 25, 12.5, 6.25, and 3.125 µM) for 24 h. As shown in Fig. 3a, AS-1 at 3.125, 6.25, and 12.5 µM showed no obvious cytotoxicity towards THP-1 monocytes. To further evaluate the anti-inflammatory potential of AS-1 in THP-1 monocytes, we assessed its inhibitory activity against LPS-activated NO production. The results demonstrated that AS-1 significantly inhibited the fluorescence intensity of NO in a dose-dependent manner (Fig. 3b,c).

### Measurement of the embryotoxicity in zebrafish treated with different concentrations of AS-1

We observed the survival rate, hatching rate, heart rate, body length, and morphological changes of zebrafish larvae treated with AS-1 for 120 h post-fertilization (hpf). At 3.125, 6.25, and 12.5 µM of AS-1, the survival rate and morphological changes of zebrafish larvae measured at different times were not significantly abnormal (Fig. 4a,b). During 48

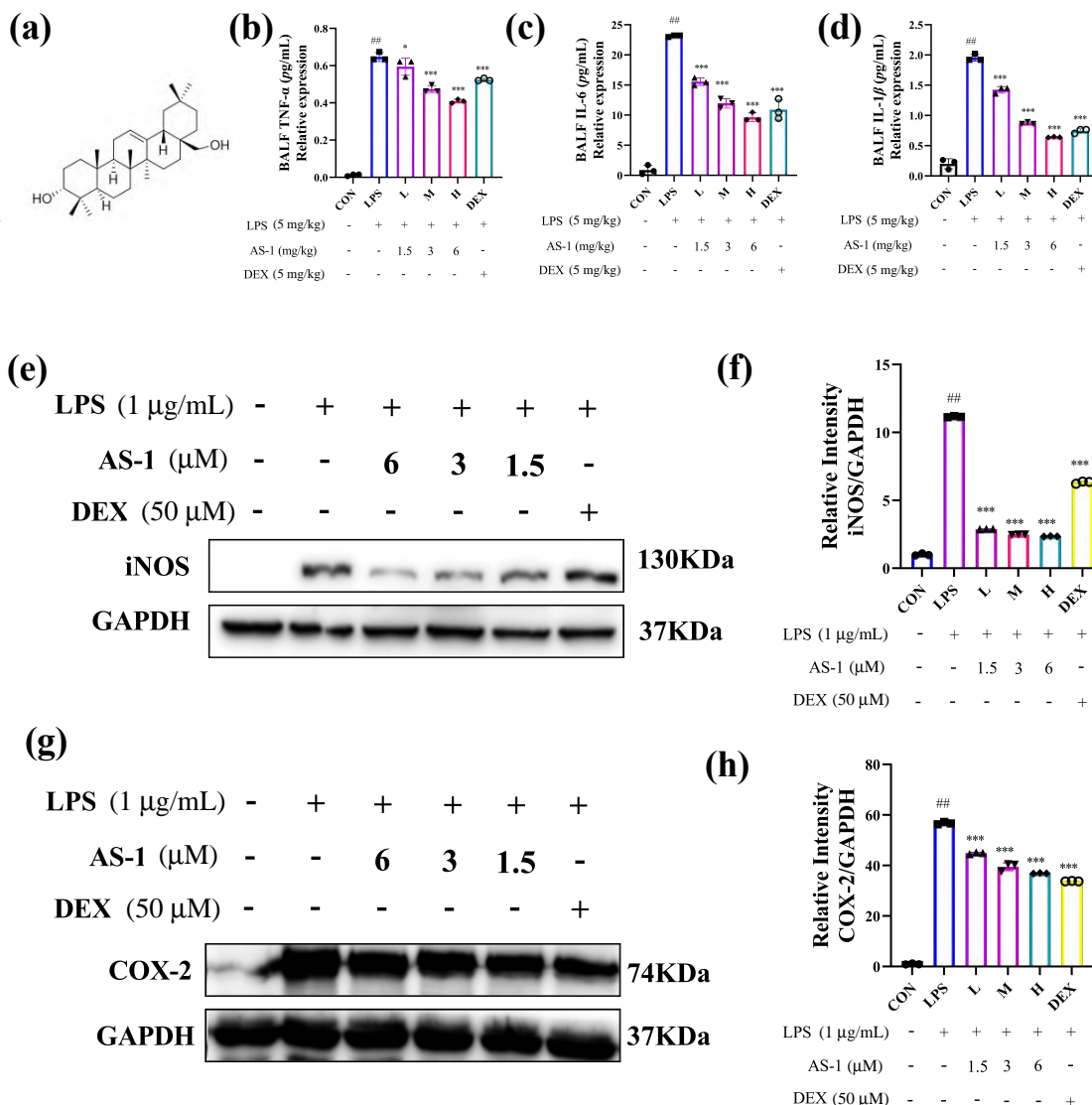


**Fig. 1** The pro-inflammation expression at different AS-1 concentrations in mouse BALF and lung tissue. (a) AS-1 chemical structure. The effect of AS-1 on the level of (b) TNF- $\alpha$ , (c) IL-6, and (d) IL-1 $\beta$  production in mouse BALF. The effect of AS-1 on (e,f) iNOS and (g,h) COX-2 protein expressions. The data are displayed as means  $\pm$  SD,  $n = 10$ . (<sup>#</sup>  $p < 0.05$  and <sup>##</sup>  $p < 0.001$  vs. the control group. \*  $p < 0.05$ , \*\*  $p < 0.01$ , and \*\*\*  $p < 0.001$  vs. the LPS group).

and 72 hpf when embryos were treated with AS-1 at 3.125, 6.25, and 12.5  $\mu$ M, we found that almost all embryos hatched into zebrafish larvae (Fig. 4c), indicating that AS-1 has no adverse effects on zebrafish hatching during development. There was no statistical difference between the 0–12.5  $\mu$ M treatment groups in body length and heart rate tests of zebrafish larvae (Fig. 4d,e).

## DISCUSSION

ALI occurs as a result of immunological recognition of the pathogen responsible for triggering a pro-

inflammatory immune response in response to severe pulmonary microbial infections [16]. It is also a major cause of tissue damage and in severe cases, irreversible lung damage can lead to death [17]. The current mainstay of treatment for ALI is the use of anti-inflammatory drugs. Non-steroidal anti-inflammatory drugs (NSAIDs) are one of the most commonly prescribed medications [18]. However, data from several experimental analyses of trials show alarmingly that NSAIDs have adverse effects on gastrointestinal, cardiovascular, hepatic, renal, cerebral, and pulmonary complications [19]. Anti-inflammatory drugs based

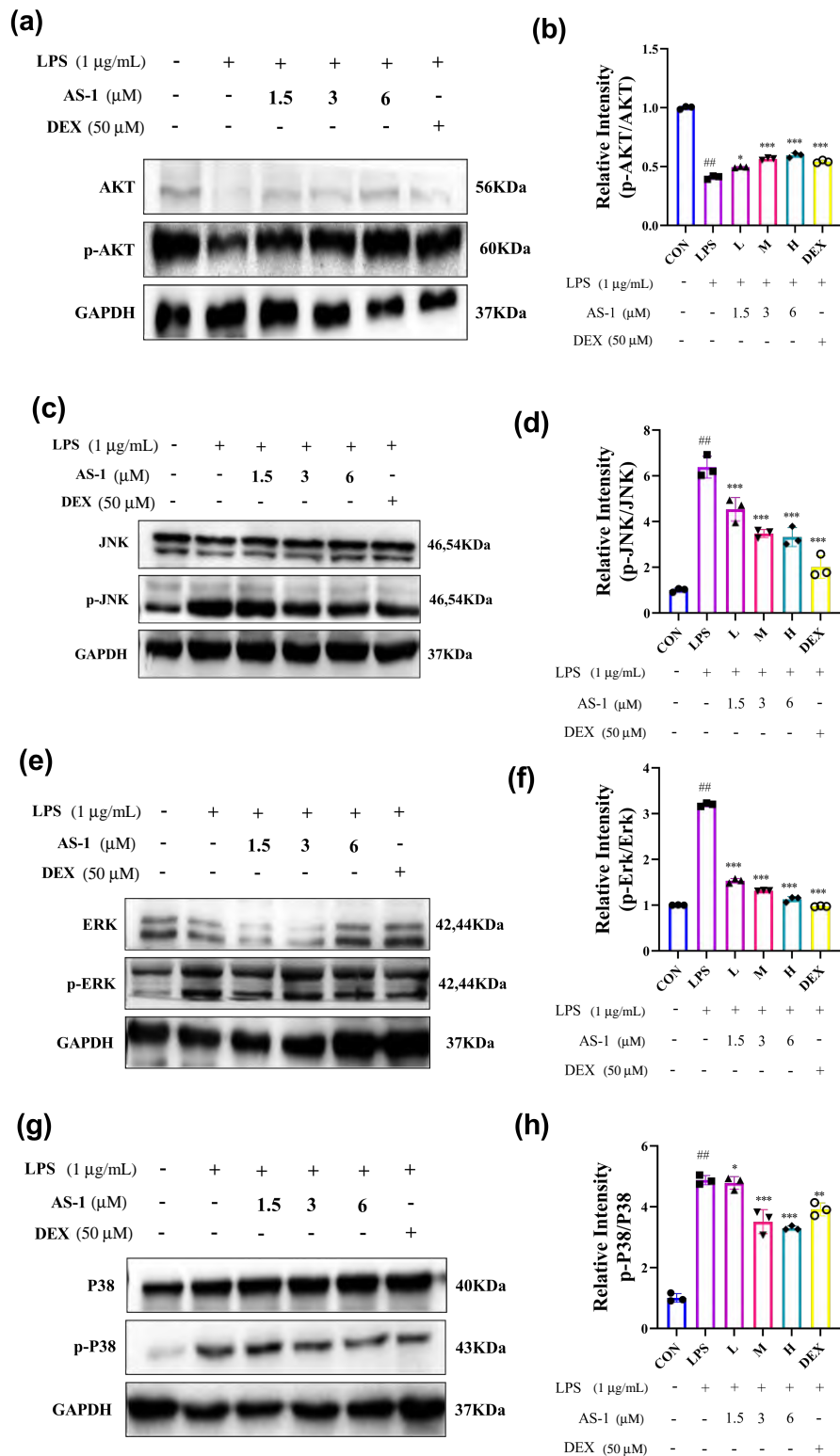


**Fig. 2** Effect of AS-1 at different concentrations on protein expression in the AKT/MAPK signaling pathways. The effect of AS-1 on (a) AKT and p-AKT, (b) JNK and p-JNK, (c) ERK and p-ERK, and (d) P38 and p-P38 protein expressions. The data are displayed as means ± SD, *n* = 10. (<sup>#</sup> *p* < 0.05 and <sup>##</sup> *p* < 0.001 vs. the control group. \* *p* < 0.05, \*\* *p* < 0.01, and \*\*\* *p* < 0.001 vs. the LPS group).

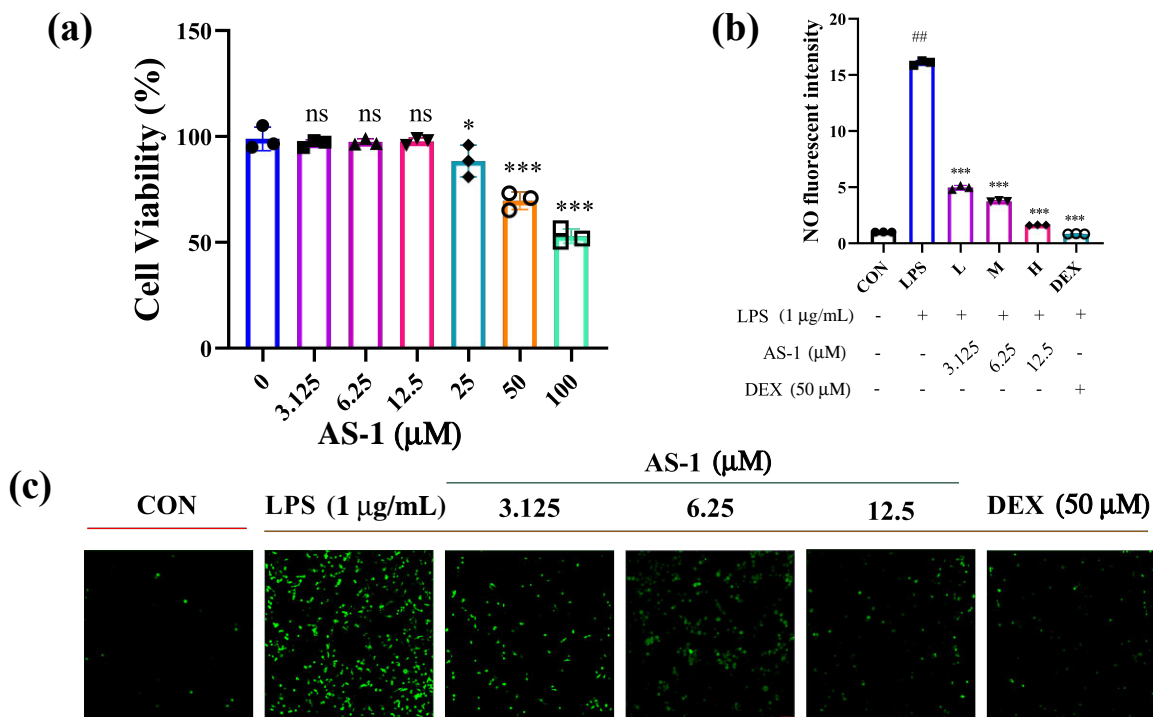


**Fig. 3** The toxicity and NO expression at different concentrations of AS-1 in THP-1 monocytes. (a) Cytotoxicity effect of AS-1 on THP-1 monocytes (b,c) Effect of AS-1 on fluorescence level of NO production in THP-1 monocytes. The data are displayed as means  $\pm$  SD,  $n = 4$ . ( $^{\#} p < 0.05$  and  $^{\#\#} p < 0.001$  vs. the control group.  $* p < 0.05$ ,  $** p < 0.01$ , and  $*** p < 0.001$  vs. the LPS group. ns = no significant difference compared to the control group.)

on Traditional Chinese Medicine (TCM) are characterized by their low toxicity and low level of side effects [20]. Flavonoids (quercetin derivatives) inhibit NF- $\kappa$ B activation and downstream pro-inflammatory cytokines (TNF- $\alpha$  and IL-6) by suppressing I $\kappa$ B $\alpha$  phosphorylation [21]. Terpenoids modulate MAPK/ERK pathways, reducing COX-2 and iNOS expression [22]. Polyphenols further enhance efficacy by scavenging reactive oxygen species (ROS) and blocking NLRP3 inflammasome assembly [23]. Preliminary studies in our laboratory found that AS-1 has a favorable anti-inflammatory effect *in vitro*. Therefore, in order to further investigate the anti-inflammatory pathway of AS-1 *in vivo*, we induced acute lung injury in mice with LPS and examined the effect of AS-1 on the expression of AKT/MAPK-related proteins in the lungs of the Balb/c mice.

LPS, an endotoxin of gram-negative bacteria, can induce ALI via AKT/MAPK mediated inflammation and is commonly used to induce ALI in animal models [24, 25]. Furthermore, LPS elicits infiltration of inflammatory cells such as neutrophils and macrophages into the injured lungs and simultaneously triggers the release of pro-inflammatory cytokines such as Prostaglandin E2 (PGE2), TNF- $\alpha$ , IL-6, and IL-1 $\beta$ ,

further aggravating inflammatory response [26]. In our study, AS-1 obviously inhibited the production of IL-6, TNF- $\alpha$ , and IL-1 $\beta$  in LPS-activated ALI mice BALF. The production of NO is regulated by the nitric oxide synthase enzyme family, in which iNOS is mainly involved [27]. In addition, COX-2 is assumed to be responsible for the synthesis of PGE2 in a range of inflammation models [28]. The present study demonstrated that AS-1 treatment downregulates iNOS and COX-2 protein expression in BALF of ALI mice, thereby suggesting the potential protective effect of AS-1 against LPS-induced inflammatory stimuli. Previous studies have revealed that the PI3K/AKT signaling pathway alters LPS-induced COX-2 and iNOS expression in ALI mice [29]. Besides, the mechanism that controls cytokines like TNF- $\alpha$  or IL-6 production in immune monocytes in response to external stimuli has been shown to involve MAPKs such as ERK and p38 as well as the AKT signaling pathway [30]. In the present study, we found reduced p-ERK, p-JNK, and p-p38 in response to AS-1 treatment, which suggested suppression of MAPK phosphorylation during LPS-induced upregulated inflammation. Recent research has highlighted that PI3K/AKT pathway activation exhibits anti-inflammatory effects [31]. Western blot

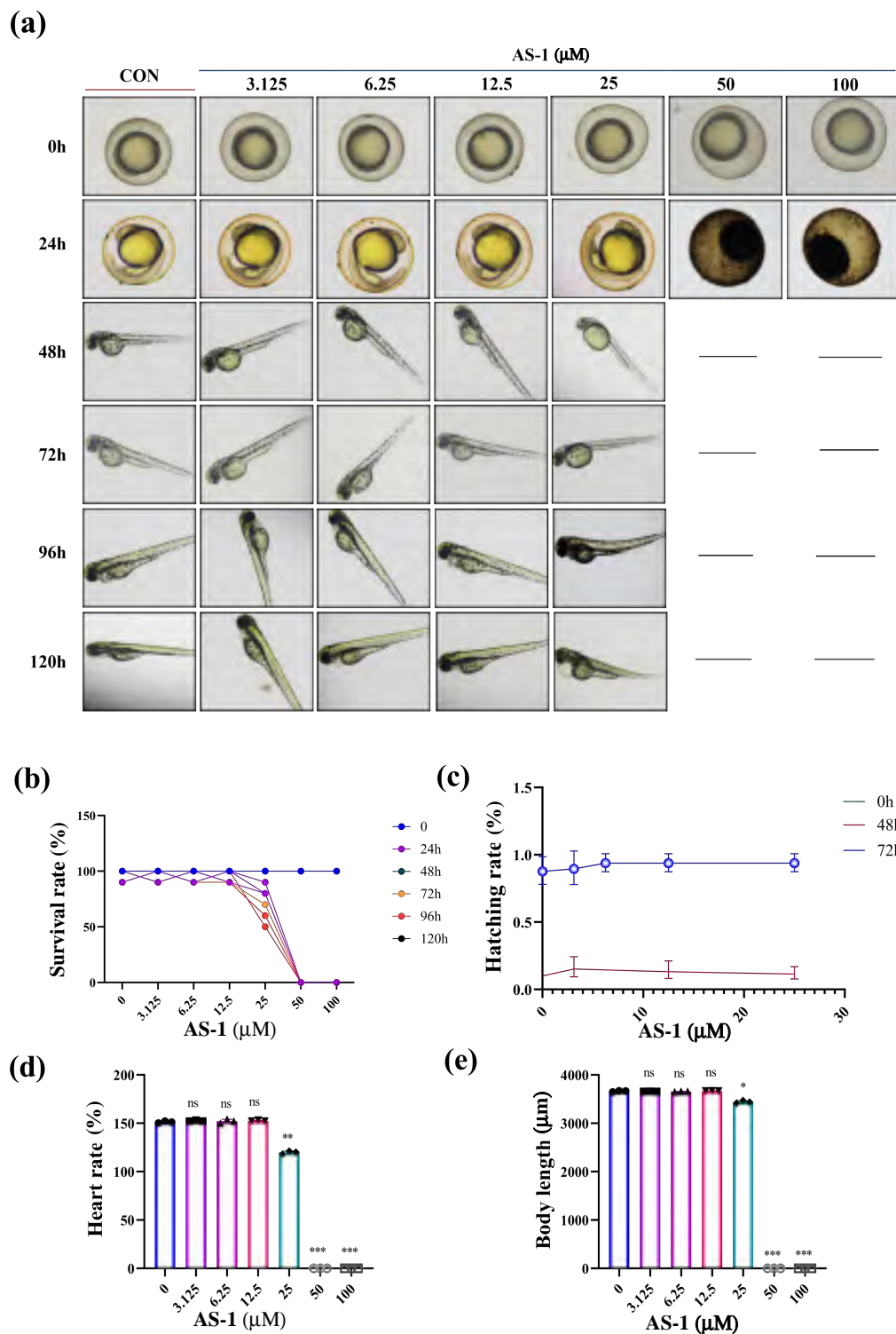


**Fig. 4** Developmental toxicity effects of AS-1 in zebrafish embryos. (a) Phenotypic changes of embryos exposed to 0–100  $\mu\text{M}$  AS-1 at 0, 24, 48, 72, 96, and 120 hpf. (b) Survival rates in zebrafish embryos exposed to 0–100  $\mu\text{M}$  AS-1 from 0 to 120 hpf. (c) Hatching rates in zebrafish embryos exposed to 0–100  $\mu\text{M}$  AS-1 at 48 and 72 hpf. (d) Heart rates in zebrafish embryos exposed to 0–100  $\mu\text{M}$  AS-1 at 96 hpf. (e) Body lengths in zebrafish embryos exposed to 0–100  $\mu\text{M}$  AS-1 at 96 hpf. The data are displayed as means  $\pm$  SD,  $n = 10$ . ( $\# p < 0.05$  and  $\#\# p < 0.001$  vs. the control group.  $* p < 0.05$ ,  $** p < 0.01$ , and  $*** p < 0.001$  vs. the LPS group, ns = no significant difference compared to the control group.)

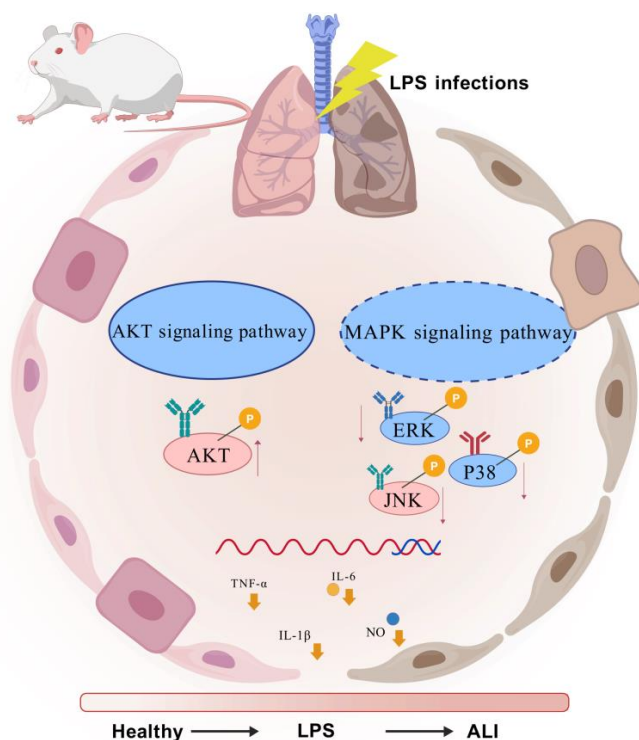


**Fig. 5** AS-1 modulating AKT/MAPK signaling pathways and suppressing inflammatory cytokines.

analysis indicated that the AKT suppression induced by LPS was activated by AS-1 in a dose-dependent manner. Overall, both *in vivo* and *in vitro* findings showed that AS-1 may protect against LPS-induced inflammation via the MAPK and AKT signaling pathways. Therefore, these results indicated that AS-1 may be a possible therapeutic candidate against ALI related to inflammation.

There is considerable evidence that macrophages are present in diseased lung tissues and are key players in the immune response to lung pathogens, contributing to the initiation of lung inflammation [32]. In the present study, we examined the toxicity and NO inhibitory activity of AS-1 on THP-1, which can be differentiated into macrophages by PMA and is widely used in research on pathogen infection and host innate immunity [33]. The results indicated that AS-1 at concentrations below 12.5  $\mu\text{M}$  had no significant toxicity to THP-1 while exhibiting excellent NO inhibitory activity.

The teratogenicity of the compound AS-1 has to be investigated, as a number of TCM, although effective, have limitations due to teratogenicity [34]. However, traditional mammalian models are costly, time-consuming, and of limited sensitivity, and *in vitro* experimental methods cannot accurately predict the biological properties of TCM *in vivo* [35]. The zebrafish is a popular vertebrate model in the field of developmental biology and has been used in toxicity studies. In

addition, zebrafish share almost 70% of their DNA sequence homology with humans and have similar neurotransmitters to humans [36]. Therefore, between cell-based assays and mammalian testing, zebrafish are used as an intermediate model organism [37]. In addition, chemical-induced malformations in zebrafish can be easily observed under a stereo microscope due to the transparent nature of their bodies [38]. In this study, we tested the effect of AS-1 on zebrafish embryos and larvae. Zebrafish deformities were observed under the microscope, and survival rate, hatchability, heart rate, and body length were used as the main detection indices. The results showed that AS-1 at 25  $\mu\text{M}$  produced teratogenic effects on zebrafish, while higher concentrations (50 and 100  $\mu\text{M}$ ) resulted in significant toxicity. In contrast, AS-1 at 12.5  $\mu\text{M}$  and below had no significant effect on survival, hatchability, heart rate, and body length of zebrafish. This experiment provides a reference basis for the subsequent comprehensive utilization and product development of AS-1.

## CONCLUSION

In summary, AS-1 inhibits the release of inflammation-related substances in BALF, further blocking the phosphorylation of MAPK-related proteins in the lung tissue of ALI mice while promoting the activation of the AKT signaling pathway. Additionally, AS-1 significantly reduces NO release in THP-1 cells. CCK-8 assays and zebrafish embryo toxicity assay indicate that AS-1 has

no significant toxicity or teratogenic effects at concentrations below 12.5  $\mu$ M. Therefore, the results of this study suggest that the anti-inflammatory effects of AS-1 can be achieved by inhibiting the MAPK signaling pathway and promoting AKT signaling pathway activation, with the concentration of 12.5  $\mu$ M or below serving as a safe dosage for its action.

### Appendix A. Supplementary data

Supplementary data associated with this article can be found at <https://dx.doi.org/10.2306/scienceasia1513-1874.2025.048>.

**Acknowledgements:** This work was supported by Fujian University of Traditional Chinese Medicine, Hainan Normal University, the Key R&D Projects in Hainan Province-Social Development (ZDYF2022SHFZ286) and National Natural Science Foundation of China [grant numbers 22177023, 22477021].

### REFERENCES

- Zhou X, Liao Y (2021) Gut-lung crosstalk in sepsis-induced acute lung injury. *Front Microbiol* **12**, 779620.
- Yang J, Li N, Zhen Y, Huang Q (2023)  $\gamma$ -Aminobutyric acid alleviates LPS-induced acute lung injury in mice through upregulating type B receptors. *Arch Med Sci* **19**, 1116–1123.
- Huynh DTN, Baek N, Sim S, Myung CS, Heo KS (2020) Minor ginsenoside Rg2 and Rh1 attenuates LPS-induced acute liver and kidney damages via downregulating activation of TLR4-STAT1 and inflammatory cytokine production in macrophages. *Int J Mol Sci* **21**, 6656.
- Park MY, Ha SE, Kim HH, Bhosale PB, Abusaliya A, Jeong SH, Park JS, Heo JD, et al (2022) Scutellarein inhibits LPS-induced inflammation through NF- $\kappa$ B/MAPKs signaling pathway in RAW264.7 cells. *Molecules* **27**, 3782.
- Li X, Cai P, Tang X, Wu Y, Zhang Y, Rong X (2024) Lactylation modification in cardiometabolic disorders: function and mechanism. *Metabolites* **14**, 217.
- Liu Z, Wang W, Luo J, Zhang Y, Zhang Y, Gan Z, Shen X, Zhang Y, et al (2021) Anti-apoptotic role of Sanhuang Xiexin Decoction and anisodamine in endotoxemia. *Front Pharmacol* **12**, 531325.
- Miao M, Yu WQ, Li Y, Sun YL, Guo SD (2022) Structural elucidation and activities of *Cordyceps militaris*-derived polysaccharides: A review. *Front Nutr* **9**, 898674.
- Zhou H, Yang T, Lu Z, He X, Quan J, Liu S, Chen Y, Wu K, et al (2023) Liquiritin exhibits anti-acute lung injury activities through suppressing the JNK/Nur77/c-Jun pathway. *Chin Med* **18**, 35.
- Long HZ, Cheng Y, Zhou ZW, Luo HY, Wen DD, Gao LC (2021) PI3K/AKT signal pathway: a target of natural products in the prevention and treatment of Alzheimer's disease and Parkinson's disease. *Front Pharmacol* **12**, 648636.
- Yee LD, Mortimer JE, Natarajan R, Dietze EC, Seewaldt VL (2020) Metabolic health, insulin, and breast cancer: why oncologists should care about insulin. *Front Endocrinol (Lausanne)* **11**, 58.
- Liu S, Flores JJ, Li B, Deng S, Zuo G, Peng J, Tang J, Zhang JH (2021) IL-20R activation via rIL-19 enhances hematoma resolution through the IL-20R1/ERK/Nrf2 pathway in an experimental GMH rat pup model. *Oxid Med Cell Longev* **2021**, 5913424.
- Daskalaki MG, Bafiti P, Kikionis S, Laskou M, Roussis V, Ioannou E, Kampranis SC, Tsatsanis C (2020) Disulfides from the brown alga *Dictyopteris membranacea* suppress M1 macrophage activation by inducing AKT and suppressing MAPK/ERK signaling pathways. *Mar Drugs* **18**, 527.
- Siddaiah C, Kumar BmA, Deepak SA, Lateef SS, Nagpal S, Rangappa KS, Mohan CD, Rangappa S, et al (2020) Metabolite profiling of *Alangium salviifolium* bark using advanced LC/MS and GC/Q-TOF technology. *Cells* **10**, 1.
- Shravya S, Vinod BN, Sunil C (2017) Pharmacological and phytochemical studies of *Alangium salviifolium* Wang. – A review. *Bull Faculty Pharm* **55**, 217–222.
- Dhruve P, Nauman M, Kale RK, Singh RP (2022) A novel hepatoprotective activity of *Alangium salviifolium* in mouse model. *Drug Chem Toxicol* **45**, 576–588.
- Zhu Y, Luo L, Zhang M, Song X, Wang P, Zhang H, Zhang J, Liu D (2023) Xuanfei Baidu formula attenuates LPS-induced acute lung injury by inhibiting the NF- $\kappa$ B signaling pathway. *J Ethnopharmacol* **301**, 115833.
- Kumar V (2020) Pulmonary innate immune response determines the outcome of inflammation during pneumonia and sepsis-associated acute lung injury. *Front Immunol* **11**, 1722.
- Kim HR, Lee SH, Noh EM, Choi B, Seo HY, Jang H, Kim SY, Park MH (2023) Therapeutic effect of enzymatically hydrolyzed cervi cornu collagen NP-2007 and potential for application in osteoarthritis treatment. *Int J Mol Sci* **24**, 11667.
- Bindu S, Mazumder S, Bandyopadhyay U (2020) Non-steroidal anti-inflammatory drugs (NSAIDs) and organ damage: A current perspective. *Biochem Pharmacol* **180**, 114147.
- Xie J, Tan P, Geng F, Shang Q, Qin S, Hao L (2023) A practical and rapid screening method for influenza virus neuraminidase inhibitors based on fluorescence detection. *Anal Sci* **39**, 547–556.
- Zhong R, Miao L, Zhang H, Tan L, Zhao Y, Tu Y, Angel Prieto M, Simal-Gandara J, et al (2022) Anti-inflammatory activity of flavonols via inhibiting MAPK and NF- $\kappa$ B signaling pathways in RAW264.7 macrophages. *Curr Res Food Sci* **5**, 1176–1184.
- Gravandi MM, Abdian S, Tahvilian M, Iranpanah A, Moradi SZ, Fakhri S, Echeverria J (2023) Therapeutic targeting of Ras/Raf/MAPK pathway by natural products: A systematic and mechanistic approach for neurodegeneration. *Phytomedicine* **115**, 154821.
- Zhang H, Tsao R (2016) Dietary polyphenols, oxidative stress and antioxidant and anti-inflammatory effects. *Curr Opin Food Sci* **8**, 33–42.
- Malisorn N, Bootkotr W, Khamkhai T, Chaikan A, Seubsasana S (2023) Celastrol attenuates interleukin-8 release from LPS-activated human monocytes and monocyte-derived macrophages by inhibiting the NF- $\kappa$ B signalling pathway. *ScienceAsia* **49**, 653–660.
- Yang Y, Ding Z, Wang Y, Zhong R, Feng Y, Xia T, Xie Y, Yang B, et al (2020) Systems pharmacology reveals the mechanism of activity of *Physalis alkekengi* L. var. *franchetii* against lipopolysaccharide-induced acute lung injury. *J Cell Mol Med* **24**, 5039–5056.
- Eng YS, Lee CH, Lee WC, Huang CC, Chang JS (2019)

- Unraveling the molecular mechanism of traditional Chinese medicine: formulas against acute airway viral infections as examples. *Molecules* **24**, 3505.
27. Huang T, Zhao D, Lee S, Keum G, Yang HO (2023) Sinaptic acid attenuates the neuroinflammatory response by targeting AKT and MAPK in LPS-activated microglial models. *Biomol Ther (Seoul)* **31**, 276–284.
  28. Budik S, Walter I, Leitner MC, Ertl R, Aurich C (2021) Expression of enzymes associated with prostaglandin synthesis in equine conceptuses. *Animals (Basel)* **11**, 1180.
  29. Jiang L, Yang D, Zhang Z, Xu L, Jiang Q, Tong Y, Zheng L (2024) Elucidating the role of *Rhodiola rosea* L. in sepsis-induced acute lung injury via network pharmacology: emphasis on inflammatory response, oxidative stress, and the PI3K-AKT pathway. *Pharm Biol* **62**, 272–284.
  30. Gao X, Zhang R, Hu F, Chen Q, Lei Z, Yang Y, Tian J, Huang L (2022) Protective effect of the Chinese herb *Draba scabra* on the sepsis myocarditis in molecular mechanism. *Evid Based Complement Alternat Med* **2022**, 2313813.
  31. Li C, Zhuo C, Ma X, Li R, Chen X, Li Y, Zhang Q, Yang L, et al (2024) Exploring the molecular targets of fingolimod and siponimod for treating the impaired cognition of schizophrenia using network pharmacology and molecular docking. *Schizophrenia (Heidelb)* **10**, 80.
  32. Öz HH, Cheng EC, Di Pietro C, Tebaldi T, Biancon G, Zeiss C, Zhang PX, Huang PH, et al (2022) Recruited monocytes/macrophages drive pulmonary neutrophilic inflammation and irreversible lung tissue remodeling in cystic fibrosis. *Cell Rep* **41**, 111797.
  33. Liu T, Huang T, Li J, Li A, Li C, Huang X, Li D, Wang S, et al (2023) Optimization of differentiation and transcriptomic profile of THP-1 cells into macrophage by PMA. *PLoS One* **18**, e0286056.
  34. Wu M, Guo C, Guo N, Zhang T, Wang Y, Wang Y, Lin X, Wu F, et al (2021) Similarity evaluation on the compound TCM formulation “Huoling Shengji Granule” and its placebo by intelligent sensory evaluation technologies and the human sensory evaluation method based on critical quality attributes. *Evid Based Complement Alternat Med* **2021**, 6637326.
  35. Mirtallo Ezzone, Anaya-Eugenio, Addo EM, Ren Y, Kinghorn AD, Carcache de Blanco (2022) Effects of Corchoroside C on NF- $\kappa$ B and PARP-1 molecular targets and toxicity profile in zebrafish. *Int J Mol Sci* **23**, 145146.
  36. Nieoczym D, Banono NS, Stępnik K, Kaczor AA, Szybowski P, Esguerra CV, Kukula-Koch W, Gawel K (2023) *In silico* analysis, anticonvulsant activity, and toxicity evaluation of Schisandrin B in zebrafish larvae and mice. *Int J Mol Sci* **24**, 12949.
  37. Park JS, Samanta P, Lee S, Lee J, Cho JW, Chun HS, Yoon S, Kim WK (2021) Developmental and neurotoxicity of acrylamide to zebrafish. *Int J Mol Sci* **22**, 3518.
  38. Wang R, Liu K, Zhang Y, Chen X, Wang X (2020) Evaluation of the developmental toxicity induced by E804 in zebrafish embryos. *Front Pharmacol* **11**, 32.

**Appendix A. Supplementary data****Table S1** Treatment status of mice.

Group	Control	Model (LPS 5 mg/kg)	LPS+DEX (5 mg/kg)	LPS+L (1.5 mg/kg)	LPS+M (3 mg/kg)	LPS+H (6 mg/kg)
Number	10	10	10	10	10	10
Treatment status	Positive	Hairiness; tardy; Increased secretion from the corners of the eyes; Respiratory abnormalities	Smoother hair; Sporadic palpebral exudation; Breathing more normally.	Hairiness; Increased secretion from the corners of the eyes; Breathing more normally.	Smoother hair; Sporadic palpebral exudation; Breathing more normally.	Smoother hair; Almost no discharge from the corners of the eyes; Breathing more normally.